

Convergent Fine-Structure Constant Using the Lambert Function

Bhatt, Ankur S. Becker, F.M.

June 22, 2022

Abstract

Here a correlation to the exact fine-structure constant is found. This derivation suggests that the fine structure constant can be theoretically determined as a Lambert function that utilizes the spectrum range of all the energy modes (radiation modes) that fit inside the observable universe between the particle horizon down to Planck Length. Alternatively, this also could be interpreted as the Lambert function of the particle horizon in natural units. Several methods use hyperbolic geometry to achieve full convergence. A compilation of various convergent equations are found to represent the fine structure constant.

1 Introduction

The fine-structure constant (FSC) is subject to multiple physical interpretations and is a recurrent topic for vivid scientific debates [4] [11]. Many attempts at a physical description which is both exact and accurate has been attempted but not yet found. The fundamental nature of the fine-structure constant has remained unclear since its discovery by A. Sommerfeld where he defined this number as the coupling factor of the electromagnetic interaction between elementary charged particles. Furthermore, it has not been clarified whether the fine-structure constant may slightly vary in spacetime [5].

This paper introduces a hypothesis that the fine structure constant depends on vacuum fluctuations and information boundaries which influence propagation paths of mass/energy and information in space and time. The nature of the FSC seems to be related to the cosmic information horizon, namely, the particle horizon and is generated due to an information horizon condition. Similar to Hawking radiation [15], it can be assumed that radiation emits from an information horizon and this establishes a wave mode cavity condition with discrete wave spectrum where allowed wavelengths fit within the nodes of the horizon confinement [19] [20]. Such radiation could be assumed to cause energy gradients in the realm of virtual particles which may indicate the establishment of forces inside the vacuum. The existence of such radiation is assumed and by

wave superposition, and an exact FSC will be derived within error bounds of the particle horizon measurement. The fundamental FSC can be mathematically derived utilizing the Lambert W -function and a simple ratio of the current size of the particle horizon and Planck length.

2 Method

2.1 Derivation of Estimated Fine Structure Constant from Uncertainty Principle

Using the uncertainty principle, it is suggested that in-between two objects, or boundary conditions, and at a defined distance, virtual particles have energy/momentum waves that are associated to Δx , and momentum, Δp . These virtual particles may transfer momentum in a confinement situation within the boundaries. Here, assuming a discrete spectrum with nodes at the horizon [4] [5], a certainty is established where the allowed waves are defined precisely for every wavelength (energy) and this corresponds to the position of the particles. Now assume there are two elementary probe charges located at the middle of the universe and edge of the observable universe, respectively, and count all the waves between these two objects. The charges of these particles are inconsequential since they will merely change the force direction and the total waves would be the same in the region. Count all the waves from Planck length, l_p , to the particle horizon radius, $R_{PH} = 4.4 \times 10^{26}$ m. The mode with the highest frequency is associated to the Planck Length while the mode with the greatest wavelength would be the particle horizon.

$$\Delta x \Delta p = \frac{\hbar}{2} \quad (1)$$

Use the energy formula for a photon $\Delta E/c = \Delta p$ and solve in terms of ΔE . One can double the energy due to two particles being considered.

$$\Delta E = \frac{\hbar c}{\Delta x} \quad (2)$$

Here $\Delta x_{max} = R_{PH}$ since the greatest uncertainty from the averaged probability of a particle in position of the superimposed wave is located in the middle of the directional span of modes.

$$\Delta E = \frac{\hbar c}{R_{PH}} \quad (3)$$

However (3) is simply the maximum distance Δx can be. Therefore, using this knowledge, plug in for $\Delta x = kl_p$ into (2) in order to count all the waves from Planck length to the circular horizon between the two probe charges up to N . The observer is positioned in the center of the universe.

$$\sum_{k=1}^N \Delta E_{tot} = \frac{\hbar c}{l_p} + \frac{\hbar c}{2l_p} + \dots + \frac{\hbar c}{Nl_p} \quad (4)$$

Looking at the summation of total waves, K , count the modes of the superimposed waves between the two charges up to N , the number of waves.

$$K = \sum_{k=1}^N \frac{1}{\Delta x} = \frac{1}{l_p} + \frac{1}{2l_p} + \dots + \frac{1}{Nl_p} \quad (5)$$

Next replace N with $\frac{R_{PH}}{l_p}$ to compute all the waves from Planck length to size of the observable universe. One can set $l_p = 1$ to use natural units.

$$K = \sum_{k=1}^{R_{PH}/l_p} \frac{1}{k} \quad (6)$$

Use the closed form approximation for a harmonic series formula namely $\sum_{k=1}^N \frac{1}{k} \approx \ln(N)$. Note, for large R_{PH} , this approximation can become an equality and also note that $\int \frac{1}{x} = \ln x$ could be used for a non-discrete method.

$$K = \ln \left(\frac{R_{PH}}{l_p} \right) \quad (7)$$

This is the total amount of waves for the energy between two information horizons. Next, do something a bit avant-garde and insert alpha, the coupling factor, as a power factor inside the equation. (The reason for this will be explained later.) Recall, α is defined as the coupling factor of the electromagnetic force between elementary particles.

$$K_{em} = \ln \left(\frac{R_{PH}}{l_p} \alpha \right) \quad (8)$$

The maximum wavelength between the two charges will have the following energy formula: $\frac{\hbar c}{R_{PH}}$. Next, divide this by the reciprocal of total waves for the electromagnetic force. Recall the formula for the electric potential for two charges is $U = \frac{k_e q_1 q_2}{r}$. This can be rewritten using $k_e = \frac{\alpha \hbar c}{e^2}$ and using two elementary charges, e , reduces to the following form $U = \frac{\hbar c \alpha}{r}$. Set $r = R_{PH}$.

$$U = \frac{\hbar c}{R_{PH}} \frac{1}{\ln \left(\frac{R_{PH}}{l_p} \alpha \right)} \quad (9)$$

Alpha can now be identified as the logarithmic ratio in the denominator.

$$\alpha = \frac{1}{\ln \left(\frac{R_{PH}}{l_p} \alpha \right)} \quad (10)$$

This nested operation is denoted as the Lambert W -function. This gives a good approximate result for the fine structure constant.

$$\frac{1}{\alpha} = W \left(\frac{R_{PH}}{l_p} \right) = 136.5389398101 \quad (11)$$

2.2 Derivation of Convergent Alpha using Hyperbolic Geometry and FLWR Metric

The approximate fine structure constant found is an interesting result as previously discovered in 2019. [6] However by investigating further, an exact solution can be found. First, let us look at some hyperbolic geometry. Note that the Gaussian curvature of a plane, κ , can be defined as the following. [1]

$$R = \frac{1}{\sqrt{-\kappa}} \quad (12)$$

Now set the curvature to the following, $\kappa = -\left(\frac{l_p}{R_{PH}}\right)^2$. This was discovered to be equivalent to the cosmological constant, Λ , which was found and could be related to the curvature of universe. [21] [24] [7]

$$R = \frac{R_{PH}}{l_p} \quad (13)$$

Next, use the hyperbolic circle circumference with radius, r . [1] Note this is the same as the curvature normalized coordinates for a radius r using Friedmann–Lemaître–Robertson–Walker (FLRW) metric.

$$s_k(r) = R \sinh \frac{r}{R} \quad (14)$$

Input $R = \frac{R_{PH}}{l_p}$ and to find to obtain the following.

$$s_k(r) = \frac{R_{PH}}{l_p} \sinh \frac{r}{R} \quad (15)$$

Finally, substitute $\frac{r}{R} = \frac{\sqrt{\phi} R_{PH}/l_p}{R_{PH}/l_p} = \sqrt{\phi}$. This could be associated to a geometric mean of two lengths ϕ and 1 from the inversion of a circle. Alternatively, it could also denote the ratio of two sides of the Kepler triangle where ϕ is the golden ratio. The Kepler triangle is apparent in Coxeter's loxodromic sequence of tangent circles. [16] It is also a convergent value in a Fibonacci sequence spiral that converges for large numbers. [2] It can also be thought of as the adjusted length of the particle horizon in natural units that is adjusted by the arc length of a hyperbolic cosine function. This would indicate a hyperbolic length. Also, this could be related to the Lorentz factor since this can be written in hyperbolic trigonometric form. [13]

$$s = \frac{R_{PH}}{l_p} \sinh \sqrt{\phi} \quad (16)$$

Below is a convergent value for the fine structure constant. As discovered in 2019 by Bhatt and Becker, it is indeed a Lambert function however a convergent value was not fully convincing until now. This further examination gives a more precise and physical approach to establish a final model. The Lambert function has been associated to time delay systems and models for projectiles with air

resistance. One could speculate that this function is a decaying function over time, e.g. a condition such as vacuum resistance.

$$\frac{1}{\alpha} = W \left(\frac{R_{PH}}{l_p} \sinh \sqrt{\phi} \right) = 137.0360071692 \quad (17)$$

Another potential representation can be written in terms of a quantized total time count of the universe in Planck time, p_t , that is adjusted to a hyperbolic geometry where the age of the universe is the following $t_U = R_H/c$. Here also one can use the relationship $R_{PH} = \frac{27}{8} R_H$. [7] (Note: Further investigation into the 27/8 factor will be addressed in the appendix.)

$$\frac{1}{\alpha} = W \left(\frac{27}{8} \frac{t_U}{p_t} \sinh \sqrt{\phi} \right) = 137.0360071692 \quad (18)$$

For a more visual approach, a Lambert function can be written as a continued fraction.

$$\frac{1}{\alpha} = \ln \frac{\frac{R_{PH}}{l_p} \sinh \sqrt{\phi}}{\ln \frac{\frac{R_{PH}}{l_p} \sinh \sqrt{\phi}}{\ln \frac{\frac{R_{PH}}{l_p} \sinh \sqrt{\phi}}{\ln \frac{\frac{R_{PH}}{l_p} \sinh \sqrt{\phi}}{\ln \frac{\frac{R_{PH}}{l_p} \sinh \sqrt{\phi}}{\ln \frac{\frac{R_{PH}}{l_p} \sinh \sqrt{\phi}}{\dots}}}}}}}} \quad (19)$$

Alternatively, one can rewrite this expression in terms of $\operatorname{arccosh}(x) = \ln(x + \sqrt{x^2 + 1})$ as the following. Note that for large x , this becomes $\operatorname{arccosh}(x) = \ln(2x)$.

$$\frac{1}{\alpha} = \operatorname{arccosh} \left(\alpha \frac{R_{PH}}{2l_p} \sinh \sqrt{\phi} \right) \quad (20)$$

A continued fraction in terms of inverse hyperbolic cosine can also be written.

$$\frac{1}{\alpha} = \operatorname{arccosh} \frac{\frac{R_{PH}}{2l_p} \sinh \sqrt{\phi}}{\operatorname{arccosh} \frac{\frac{R_{PH}}{2l_p} \sinh \sqrt{\phi}}{\operatorname{arccosh} \frac{\frac{R_{PH}}{2l_p} \sinh \sqrt{\phi}}{\operatorname{arccosh} \frac{\frac{R_{PH}}{2l_p} \sinh \sqrt{\phi}}{\operatorname{arccosh} \frac{\frac{R_{PH}}{2l_p} \sinh \sqrt{\phi}}{\dots}}}}}}}} \quad (21)$$

This has significant accuracy that converges to the value of the experimental FSC of $1/\alpha_{exp} = 137.0359990837$ [22]. This theoretical fine-structure constant has an error of approximately 5.9×10^{-8} with respect to the experimental value. [22].

2.3 Fine Structure Constant Connection to Primes

Another observation suggests that the FSC could be related to the primes. First, let us speculate that the Basel function is related to the probability that two numbers are relatively prime. By inserting the probability of this, which is the well known second order zeta function, $\zeta(2) = \frac{\pi^2}{6}$, one can obtain a fairly accurate convergent FSC based on error bounds of the particle horizon length. (Interestingly, $\sinh \sqrt{\phi}$ is almost identical in value to $\frac{\pi^2}{6}$.)

$$\frac{1}{\alpha} = W \left(\frac{\pi^2 R_{PH}}{6 l_p} \right) = \mathbf{137.0366179652} \quad (22)$$

The sum of reciprocal primes has a divergent series but is bounded by the following for large n .

$$\sum_{p \leq n} \frac{1}{p} \leq \ln \ln(n+1) - \ln \left(\frac{\pi^2}{6} \right) \quad (23)$$

Substitute in for $n = R_{PH}/l_p$ into the above equation and subtract from the total wave mode count $\ln(R_{PH}/l_p)$.

$$\frac{1}{\alpha} = \ln \left(\frac{R_{PH}}{l_p} \right) - \ln \ln \left(\frac{R_{PH}}{l_p} \right) + \ln \left(\frac{\pi^2}{6} \right) = 137.0048725519 \quad (24)$$

Keep the same substitution above but add the $\sinh \sqrt{\phi}$ term from the previous section.

$$\frac{1}{\alpha} = \ln \left(\frac{R_{PH}}{l_p} \sinh \sqrt{\phi} \right) - \ln \ln \left(\frac{R_{PH}}{l_p} \sinh \sqrt{\phi} \right) + \ln \left(\frac{\pi^2}{6} \right) = 137.4984322127 \quad (25)$$

This might seem like merely a mathematical exercise but for large n the Lambert function is the following.

$$W = \ln n - \ln \ln(n) + o(1) \quad (26)$$

By ignoring the error term and inputting the substitution found for the numerical FSC one gets a very similar value to the total waves subtracted from the primes approach. [26]

$$\frac{1}{\alpha} = \ln \left(\frac{R_{PH}}{l_p} \sinh \sqrt{\phi} \right) - \ln \ln \left(\frac{R_{PH}}{l_p} \sinh \sqrt{\phi} \right) = 137.0007319102 \quad (27)$$

$$\frac{1}{\alpha} = \ln \left(\frac{\pi^2 R_{PH}}{6 l_p} \right) - \ln \ln \left(\frac{\pi^2 R_{PH}}{6 l_p} \right) = 137.0013603953 \quad (28)$$

This may suggest that the Lambert function and the FSC could physically represent the number of prime waves subtracted from total number of waves. Here a prime wave could be considered a fundamental wave without a Fourier spectrum and one may speculate that this could be related to nesting of energies (see the continuous fraction aspect of the model).

3 Discussion

As outlined in Table 1, below is the error between the experimental and theoretical FSC. The deviations can be attributed to the error in the exact particle horizon measurement. For example, by using the value $4.3999644255 \times 10^{26}$ m this gives an exact value for the FSC for equation (17).

Geometric visualizations may correlate the dimensionless value of the fine structure constant to a hyperbolic geometry (e.g. tiling a hyperbolic space with dodecahedron elements). These figures are available in the appendix of this document.

Figure 7 in the appendix may correlate to Haug's work where a pair of fundamental Planck scale particles, which may be a part of vacuum fluctuations, could have a longitudinal oscillation characteristic. [14] One may speculate that these could be projected into a scenario where the propagated path of the logarithmic spiral is linked to the trajectory and span between particles within the established quantum vacuum oscillations.

Various illustrations are compiled to inspire and facilitate future research including the aspect that the golden ratio may evolve as an expanding vortex-like scenario which is projected between different frames with different curvature properties. Here the hyperbolic frame is of particular interest.

Looking into these highly convergent results, additional questions arise including the consideration that a slight variation in the fine structure constant with time may vary in value. This would be under the condition that other fundamental constants during Hubble horizon expansion are entirely constant or may only slightly vary in value (such as the gravitational constant G correlated to the definition of the Planck length scale).[25] It is also already well known that the fine structure constant can vary with different acceleration conditions and it varies with energy. For example, the energy associated to the mass of the W -boson the fine structure value is approximately $1/128$. [12] [23] Future research may clarify these conditions.

Current ongoing research and results indicate a potential variation of G . One may speculate that there might be a not yet understood mechanism that influences the Planck length value over eons of time and space. Some variations in the range of few percents in G have been identified in the past. [10] [27] [17] G may influence the Planck value. This might keep the FSC more stable from a math perspective.

Table 1: Error Table

Equation Number	Equation	Error - Experimental FSC
17	$W\left(\frac{R_{PH}}{l_p} \sinh \sqrt{\phi}\right)$	5.9×10^{-8}
22	$W\left(\frac{\pi^2 R_{PH}}{6 l_p}\right)$	4.7×10^{-6}
24	$\ln\left(\frac{R_{PH}}{l_p}\right) - \ln \ln\left(\frac{R_{PH}}{l_p}\right) + \ln\left(\frac{\pi^2}{6}\right)$	2.3×10^{-4}
25	$\ln\left(\frac{R_{PH}}{l_p} \sinh \sqrt{\phi}\right) - \ln \ln\left(\frac{R_{PH}}{l_p} \sinh \sqrt{\phi}\right) + \ln\left(\frac{\pi^2}{6}\right)$	3.4×10^{-3}
27	$\ln\left(\frac{R_{PH}}{l_p} \sinh \sqrt{\phi}\right) - \ln \ln\left(\frac{R_{PH}}{l_p} \sinh \sqrt{\phi}\right)$	2.6×10^{-4}
28	$\ln\left(\frac{\pi^2 R_{PH}}{6 l_p}\right) - \ln \ln\left(\frac{\pi^2 R_{PH}}{6 l_p}\right)$	2.5×10^{-4}
11	$W\left(\frac{R_{PH}}{l_p}\right)$	3.6×10^{-3}

4 Conclusion

These findings provide an opportunity to review the fine structure constant from a new and novel perspective by taking into account hyperbolic space and the correlated vacuum fluctuations that act between the particles.

This document is dedicated to guide future research. These suggested initial correlations provide a novel hypothesis to associate the fine structure constant to vacuum fluctuations and Planck scale using a confinement situation where growth is towards the cosmic information horizon boundary.

5 Appendix

5.1 Connecting the Particle Horizon & Hubble Radius to the Golden Ratio

From research by Bhatt and Becker from 2019, the relationship of the Hubble radius and particle horizon radius was found to be $R_{PH} = 27/8R_H$ from the Friedmann equations. [7] However, one may speculate that a more simplistic and perhaps convincing approach, using hyperbolic geometry which can also be interpreted as the Lorentz formula, might give some insight to where this value comes from. First recall the formula for rapidity. [9]

$$\gamma = \cosh w = \frac{1}{\sqrt{1 - \frac{v^2}{c^2}}} \quad (29)$$

By setting the rapidity value of $w = \frac{3\pi}{5}$, which is a type of golden angle, one

can almost obtain the 27/8 factor.

$$\gamma = \cosh \frac{3\pi}{5} = \frac{27}{8} \quad (30)$$

It was also found that this is almost equivalent to the following: $\operatorname{arctanh} \frac{3}{\pi} = \frac{3\pi}{5}$. Therefore, one can rewrite (30). Here $3/\pi$ is directly related to ratio of the velocity and speed of light.

$$\gamma = \frac{1}{\sqrt{1 - (\frac{3}{\pi})^2}} = \frac{27}{8} \quad (31)$$

Further investigation led to the finding that the ratio of the famous golden angle $\pi(3 - \sqrt{5})$, often recognized as approximately 137.5 degrees, and $\sqrt{\phi}$, from the Kepler triangle, gives essentially a convergent value to 27/8. This can also be written as the hyperbolic cosine of the circumference with radius of $\frac{1}{\phi^{2.5}}$. This could be a normalized value using ϕ^2 as the scale reduction factor. Both the diagonal of a dodecahedron between faces as well as the spiral length of infinite pentagons with maximum side size of 1, both have lengths of ϕ^2 . [3] Potential geometric representations are shown in the next appendix section.

$$\gamma = \cosh \frac{\pi(3 - \sqrt{5})}{\sqrt{\phi}} = \cosh \frac{2\pi}{\phi^{2.5}} = \frac{27}{8} \quad (32)$$

This can be rewritten as the subtraction of two Kepler triangle angles with a scale growth factor of ϕ between them.

$$\gamma = \cosh \left(\frac{2\pi}{\sqrt{\phi}} - \frac{2\pi}{\phi\sqrt{\phi}} \right) = \frac{27}{8} \quad (33)$$

One can rewrite the FSC Lambert equation (17) using R_H as the hubble radius.

$$\frac{1}{\alpha} = W \left(\frac{R_H}{l_p} \cosh \frac{2\pi}{\phi^{2.5}} \sinh \sqrt{\phi} \right) \quad (34)$$

Another approach assumes proper acceleration for a 1+1 flat spacetime. Here proper acceleration is $a_p = \gamma_p^3 a$. The exact value of $\frac{3}{2}$ was found using the golden ratio. By using the logarithmic term this could be seen as a Poincare arc length.

$$\gamma_p = \cosh(\ln(\phi^2)) = \frac{3}{2} \quad (35)$$

By reducing the hyperbolic cosine and logarithmic operation one can rewrite this as a simple relationship. This could be seen as the average of two lengths or distances between lengths.

$$\gamma_p = \frac{1}{2} (\phi^2 + \phi^{-2}) = \frac{3}{2} \quad (36)$$

Finally, another interesting correlation to this special factor was found by using the golden spiral on two axes while placing time on the third axis. The following parametric equation for golden spiral was used where the golden ratio growth factor is the following: $b = \frac{\ln \phi}{\pi/2}$. [18]

$$\begin{cases} x = e^{bt} \cos t \\ y = e^{bt} \sin t \\ z = t \end{cases} \quad (37)$$

Compute the arc length of this curve from 0 to 2π which results in close convergence.

$$s(2\pi) = \int_0^{2\pi} \sqrt{x'(t)^2 + y'(t)^2 + z'(t)^2} dx = 2\pi \left(\frac{27}{8} \right) \quad (38)$$

Below is the error between the computed γ compared to the assumed value of $\frac{27}{8}$.

Table 2: Error Table for $\frac{27}{8}$

Equation Number	Equation γ	Error from $\frac{27}{8}$
30	$\cosh \frac{3\pi}{5}$	1.8×10^{-3}
31	$\frac{1}{\sqrt{1 - (\frac{3}{\pi})^2}}$	1.8×10^{-3}
32,33	$\cosh \frac{\pi(3-\sqrt{5})}{\sqrt{\phi}}, \cosh \frac{2\pi}{\phi^{2.5}}, \cosh \left(\frac{2\pi}{\sqrt{\phi}} - \frac{2\pi}{\phi\sqrt{\phi}} \right)$	9.6×10^{-5}
38	$\frac{s(2\pi)}{2\pi}$	8.5×10^{-4}

5.2 Geometric Visualizations of the Fine Structure Constant

Below are various suggested models and illustrations that could help with visualization of the fine structure constant. A few equations listed here might be relevant to the images below. The first shows a connection between the Kepler triangle and the pentagon/decahedron. The second equation shows Planck's constant and it's relationship to Planck length, the golden ratio and the pentagon/decahedron. [8]. The equations have errors of 3.0×10^{-4} and 7.9×10^{-5} respectively.

$$\frac{\frac{2\pi/5}{\arcsin \frac{1}{\phi}}}{\frac{2\pi/5}{\phi^{2.5}}} = \frac{5 \arcsin \frac{1}{\phi}}{\phi^{2.5}} = 1 \quad (39)$$

$$\hbar = \frac{5l_p \sinh \sqrt{\phi}}{\phi^2 \ln \phi} = \frac{5l_p \sinh \sqrt{\phi}}{\phi^2 \operatorname{arcsinh} \frac{1}{2}} \quad (40)$$

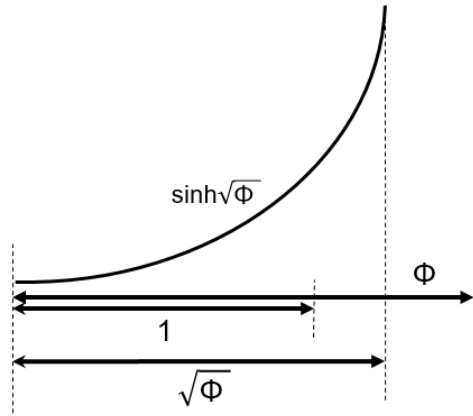


Figure 1: Hyperbolic Sine Length and Golden Ratio

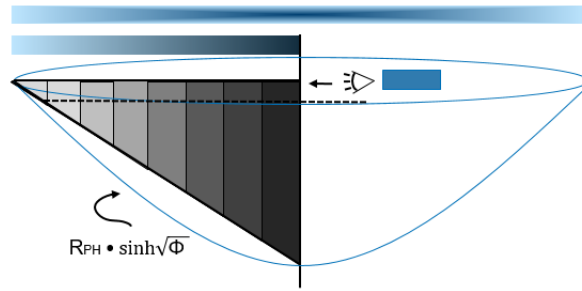


Figure 2: Particle Horizon Hyperbolic Distance With Kepler Triangles

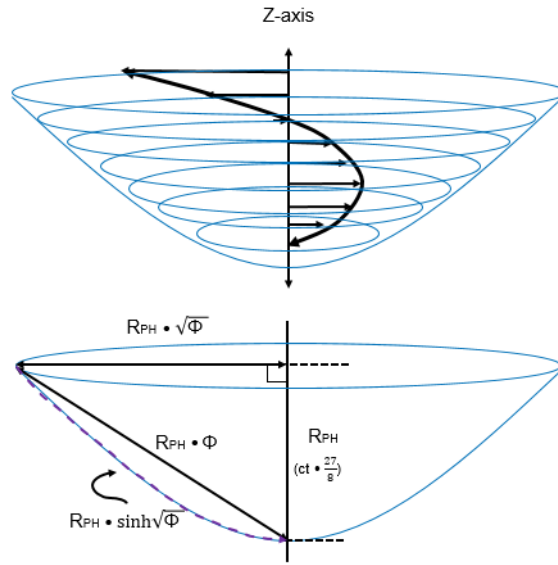


Figure 3: Spiral Path

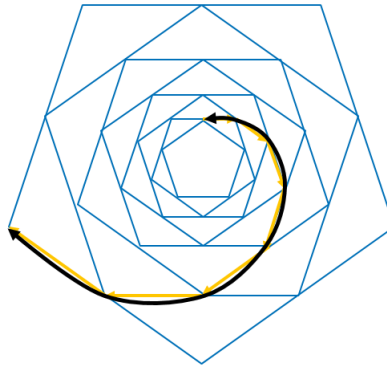


Figure 4: Nested Pentagon Spiral

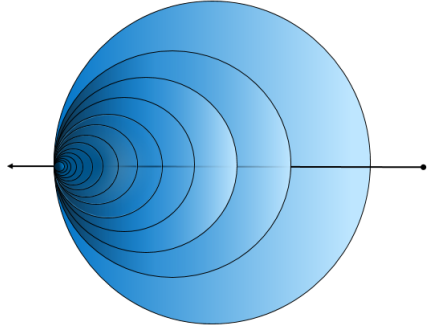


Figure 5: Continuous Nested Fraction Ratio

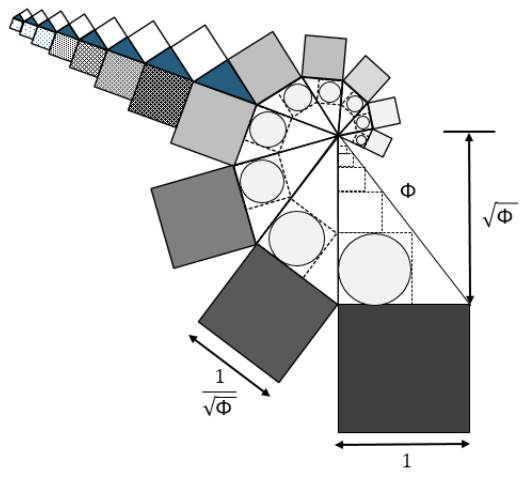


Figure 6: Kepler Triangle Golden Spiral

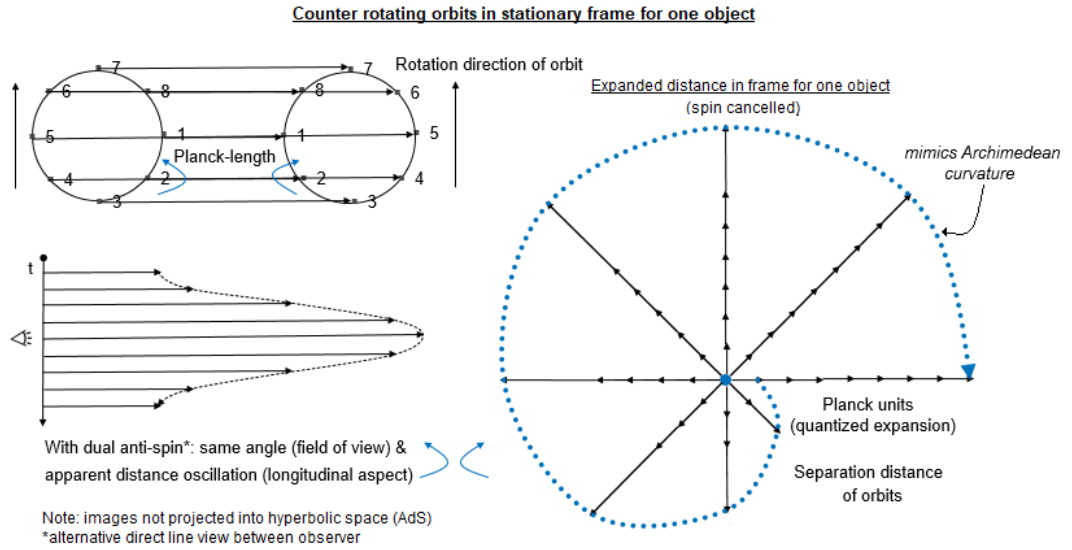


Figure 7: Quantized Expanded Distance 1

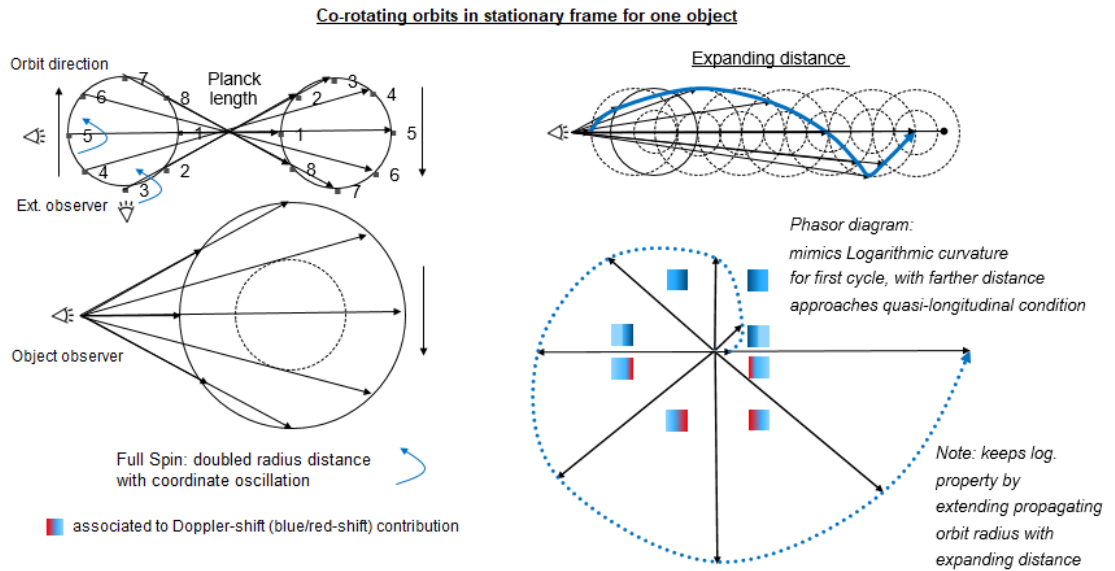


Figure 8: Quantized Expanded Distance 2

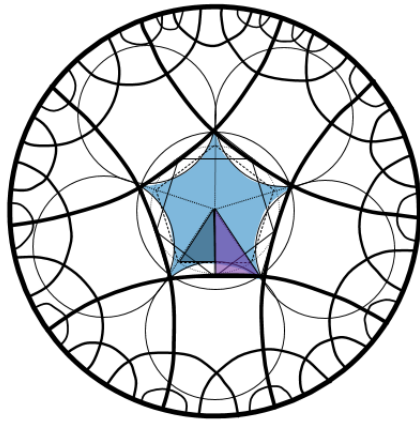


Figure 9: Hyperbolic Pentagon 1

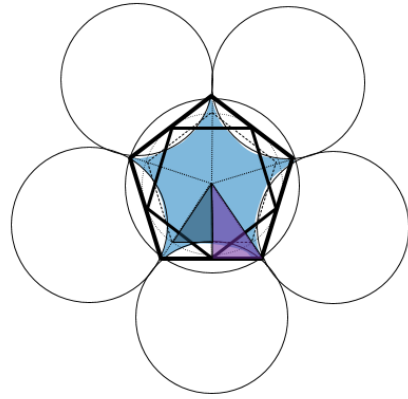


Figure 11: Hyperbolic Pentagon 3

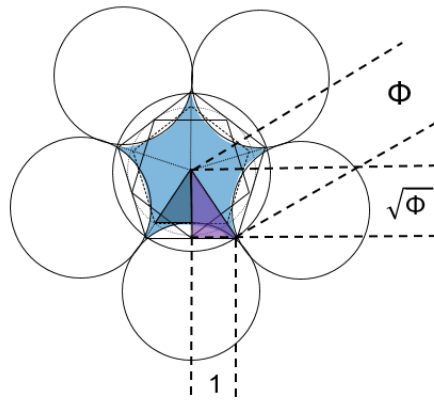


Figure 10: Hyperbolic Pentagon 2

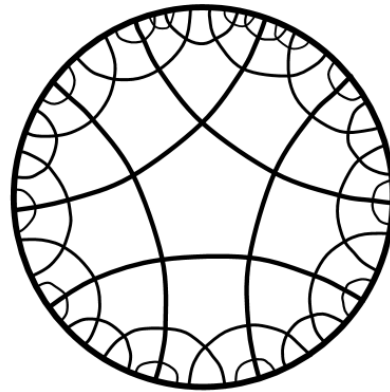


Figure 12: Hyperbolic Pentagon Tiling

References

- [1] Hyperbolic geometry. https://en.wikipedia.org/wiki/Hyperbolic_geometry.
- [2] Phi and fibonacci in kepler and golden triangles. <https://www.goldennumber.net/triangles>.
- [3] Polygon spiral. <http://jwilson.coe.uga.edu/EMAT6680Fa09/KimS/EMAT6690/Essay2/P1.html>.
- [4] S. L. Adler. Theories of the fine structure constant alpha. 1972.
- [5] J. D. Bekenstein and M. Schiffer. Varying fine structure “constant” and charged black holes. *Phys. Rev. D*, 80:123508, Dec 2009.
- [6] A. S. Bhatt and F. M. Becker. Correlation of the fine-structure constant to the cosmic horizon and planck length. *vixra.org*, page 8, 2019.
- [7] A. S. Bhatt and F. M. Becker. Emergent cosmological constant from a holographic mass/energy distribution. *vixra.org*, page 13, 2019.
- [8] A. S. Bhatt and F. M. Becker. An equation relating planck length, planck’s constant and the golden ratio. *vixra.org*, page 2, 2021.
- [9] P. Chalmoviansky. Basic facts on hyperbolic geometry and its applications. *G - Slovenský Časopis pre Geometriu a Grafiku*, 8, 01 2011.
- [10] H. Desmond, J. Sakstein, and B. Jain. Five percent measurement of the gravitational constant in the large magellanic cloud. *Physical Review D*, 103, 01 2021.
- [11] R. Feynman. *Q E D*:. Penguin Books. Penguin, 1990.
- [12] H. Fritzsche. *Fundamental Constants at High Energy*, pages 89–95. 11 2007.
- [13] E. G. Haug. The lorentz transformation at the maximum velocity for a mass. *viXra*, 2016.
- [14] E. G. Haug. Collision-space-time: Unified quantum gravity. *Physics Essays*, 33(1):46–78, 2020.
- [15] S. W. Hawking. Evaporation of two-dimensional black holes. *Phys. Rev. Lett.*, 69:406–409, Jul 1992.
- [16] J. Kocik. A note on unbounded apollonian disk packings, 2019.
- [17] A. Kordi. Variation of the gravitational constant with time in the framework of the large number and creation of matter hypothesizes. *Journal of King Saud University - Science*, 21:151–154, 07 2009.
- [18] C. Lăzureanu. Spirals on surfaces of revolution. *VisMath*, 16:1–10, 12 2014.

- [19] M. McCulloch. Inertia from an asymmetric casimir effect. *EPL (Europhysics Letters)*, 101, 02 2013.
- [20] M. E. McCulloch. Minimum accelerations from quantised inertia. *EPL (Europhysics Letters)*, 90(2):29001, 2010.
- [21] M. E. McCulloch and J. Giné. Modified inertial mass from information loss. *Modern Physics Letters A*, 32(28):1750148, 2017.
- [22] P. J. Mohr, D. B. Newell, and B. N. Taylor. Codata recommended values of the fundamental physical constants: 2014. *Rev. Mod. Phys.*, 88:035009, Sep 2016.
- [23] S. Sannikov. Renormalization of the fine structure constant at high energies. *Russian Physics Journal*, 39(1):1–8, 1996.
- [24] M. Sheppeard. The algebra of non local neutrino gravity. 01 2018.
- [25] A. Unzicker. On the origin of the constants c and h . <http://vixra.org/abs/1508.0170>, 08 2015.
- [26] M. Visser. Primes and the lambert w function. *Mathematics*, 6(4), 2018.
- [27] W. Zhao, B. Wright, and B. Li. Constraining the time variation of newton’s constant g with gravitational-wave standard sirens and supernovae. *Journal of Cosmology and Astroparticle Physics*, 2018, 04 2018.